UNCERTAINTY ANALYSIS OF A SIMPLE FRINGE PROJECTION SYSTEM

Shawn Moylan and Gregory Vogl
Manufacturing Engineering Laboratory
National Institute of Standards and Technology (NIST)[1]
Gaithersburg, Maryland, USA

INTRODUCTION

The "holy grail" in durable goods manufacturing is elimination of the need for off-line part inspection. Fringe projection [1-4] is an attractive process for on-machine metrology because the flexibility of the setup and the relative long working distances of the system's components help address several of the challenges associated with on-machine metrology. Specifically, the system components can remain on the machine throughout the machining process and can measure the entire part without machine movement. These help de-couple the uncertainty in the machine tool from the uncertainty in the measurement process.

Literature review on fringe projection indicates a thorough uncertainty analysis is absent. The current work addresses this need, discussing the challenges encountered in the analysis. The results provide much more than just a standard uncertainty value for the current on-machine setup at the National Institute of Standards and Technology (NIST). Rather, the uncertainty analysis serves as a tool to improve several aspects of the process, most notably the calibration process.

MATHEMATICAL FOUNDATION

Fringe projection belongs to the field of stereophotogrammetry, which uses two-dimensional data from multiple coordinate systems to obtain results with an added dimension in a target coordinate system. Two or more two-dimensional camera images from different perspectives of the same real-world scene have correspondence points allowing determination, through solution of the stereo correspondence problem, of three-dimensional coordinates of the surface in the captured scene [5]. Fringe projection allows automated determination of correspondence points by replacing one of the cameras with a projector that projects a known pattern onto the scene. Thus, in a typical fringe projection system, two-dimensional data from the camera and projector coordinate frames provide three-dimensional data in the real-world coordinate frame. However, to ease analysis and understanding, the current study examines a simpler system with one-dimensional camera and projector data and two-dimensional real-world data.

Points in one coordinate frame can be expressed in another coordinate frame through homogeneous transformation matrices:

$$\begin{bmatrix} hx_c \\ h \end{bmatrix} = \begin{bmatrix} C_{11} & C_{12} & C_{13} \\ C_{21} & C_{22} & C_{23} \end{bmatrix} \begin{bmatrix} x_R \\ z_R \\ 1 \end{bmatrix} \quad (1a)$$

$$\begin{bmatrix} wx_p \\ w \end{bmatrix} = \begin{bmatrix} P_{11} & P_{12} & P_{13} \\ P_{21} & P_{22} & P_{23} \end{bmatrix} \begin{bmatrix} x_R \\ z_R \\ 1 \end{bmatrix} \quad (1b)$$

where x_R and z_R are coordinates in the real-world coordinate frame, x_c and x_p are the x-coordinates in the camera and projector coordinate frames, respectively, and h and w are scale factors. C_{ij} and P_{ij} are transformation matrix components expressing real-world coordinates in the camera and projector coordinate frames. Expanding and rearranging Eqs. (1), we obtain:

$$C_{11}x_R + C_{12}z_R + C_{13} - C_{21}x_R x_c - C_{22}z_R x_c - C_{23}x_c = 0 \quad (2a)$$

$$P_{11}x_R + P_{12}z_R + P_{13} - P_{21}x_R x_p - P_{22}z_R x_p - P_{23}x_p = 0 \quad (2b)$$

Notice that if x_c, x_p, C_{ij}, and P_{ij} are known, there are two equations to solve for the two unknowns x_R and z_R. The equations can be rearranged into matrix form to reflect this:

$$\begin{bmatrix} C_{11} - C_{21}x_c & C_{12} - C_{22}x_c \\ P_{11} - P_{21}x_p & P_{12} - P_{22}x_p \end{bmatrix} \begin{bmatrix} x_R \\ z_R \end{bmatrix} = \begin{bmatrix} C_{23}x_c - C_{13} \\ P_{23}x_p - P_{13} \end{bmatrix} \quad (3)$$

Thus, the output quantities of x_R and z_R depend on the input quantities x_c, x_p, C_{ij} and P_{ij}. Uncertainties in the output quantities are

[1] Official contribution of the National Institute of Standards and Technology; not subject to copyright in the United States.

functions of the uncertainties in the input quantities [6]. C_{ij} and P_{ij} are determined through a prior calibration.

CALIBRATION

When the fringe projection system is first setup, the camera and projector transformation matrix components are unknown. These components can be estimated using a calibration artifact with known real-world coordinates. The discussion below concentrates on the camera calibration, but can also be applied to the projector.

Examining Eq. 2a, one can see that there are 6 unknown C_{ij}. Because the $[C_{ij}]$ matrix is a homogenous transformation matrix, C_{23} is set equal to 1 for a unique solution. Thus, at least five real-world coordinates and the corresponding camera coordinates must be known to estimate the unknown C_{ij}.

If there are $N > 5$ known non-collinear real-world coordinates, then C_{ij} can be estimated by a least-squares method. N known real-world coordinates yield N equations similar to Eq. (2a):

$$\begin{bmatrix} x_{a_1} & z_{a_1} & 1 & -x_{a_1}x_{c_1} & -z_{a_1}x_{c_1} \\ x_{a_2} & z_{a_2} & 1 & -x_{a_2}x_{c_2} & -z_{a_2}x_{c_2} \\ \vdots & \vdots & \vdots & \vdots & \vdots \\ x_{a_n} & z_{a_n} & 1 & -x_{a_n}x_{c_n} & -z_{a_n}x_{c_n} \end{bmatrix} \begin{bmatrix} C_{11} \\ C_{12} \\ C_{13} \\ C_{21} \\ C_{22} \end{bmatrix} = \begin{bmatrix} x_{c_1} \\ x_{c_2} \\ \vdots \\ x_{c_n} \end{bmatrix} \quad (4)$$

where x_{a_i} and z_{a_i} are known calibration artifact coordinates. Notice that Eq. (4) takes the form $\boldsymbol{AC} = \boldsymbol{y}$. This means least squares estimates for $\boldsymbol{C}$ can be found by solving the normal equations:

$$\boldsymbol{C} = \left(\boldsymbol{A}^T\boldsymbol{A}\right)^{-1}\boldsymbol{A}^T\boldsymbol{y} \quad (5)$$

Note that equations similar to Eqs. (4) and (5) exist for the projector and its P_{ij} values.

DIFFICULTIES WITH UNCERTAINTY

Though estimates for the transformation matrix components follow the above well-known approach, determination of the uncertainties in those components is not so straightforward. Ordinarily the standard uncertainties in fit values are determined by calculating the components' covariance matrix. However, this approach to uncertainty determination assumes all the uncertainty comes from the $\boldsymbol{y}$ vector and the $\boldsymbol{A}$ matrix is known exactly.

In this case, there is also uncertainty in the components of the $\boldsymbol{A}$ matrix. Specifically, the standard uncertainties in the known real-world coordinates on the artifact come from a calibration certificate for the artifact (type B uncertainty). The standard uncertainty in the camera coordinates come from a statistical analysis of the edge detection process (type A uncertainty). Additionally, when determining the combined standard uncertainty $u(x_R)$, there will be significant correlation between $u(C_{ij})$ and $u(x_c)$ that may be difficult to determine.

To avoid these issues, C_{ij} are left in equation form, so that x_R and z_R are explicit functions of all calibration values and part measurements. However, due to the complexity of the equations, the only way to express them is with mathematical software capable of symbolic manipulation.

ANALYSIS

After substituting the equations for C_{ij} and P_{ij} into Eq. (3), the output quantities x_R and z_R depend only on camera coordinates x_c, projector coordinates x_p, and calibration artifact coordinates x_a and z_a as input quantities. Of note is that these input quantities are all independent. Thus, as defined by reference [6], the combined standard uncertainty in the x-coordinate is:

$$u(x_R) = \left[\sum\left(\frac{\partial x_R}{\partial x_i}\right)^2 u^2(x_i)\right]^{1/2} \quad (6)$$

where $\partial x_R/\partial x_i$ is the sensitivity coefficient for each input quantity, and $u(x_i)$ are standard uncertainty values for the input quantities.

Mathematical software is capable of determining all sensitivity coefficients symbolically:

$$\begin{aligned} u(x_R) = \Bigg\{ &\left(\frac{L_c}{l_c}\right)^2 \left[\left(V_{x_c}\,u(x_c)\right)^2 + \left(V_{x_c}^{cal}\,u(x_c)\right)^2\right] \\ &+ \left(\frac{L_p}{l_p}\right)^2 \left[\left(V_{x_p}\,u(x_p)\right)^2 + \left(V_{x_p}^{cal}\,u(x_p)\right)^2\right] \\ &+ \left(V_{x_R}^{cal}\,u(x_a)\right)^2 + \left(V_{z_R}^{cal}\,u(z_a)\right)^2 \Bigg\}^{1/2} \end{aligned} \quad (7a)$$

$$\begin{aligned} u(z_R) = \Bigg\{ &\left(\frac{L_c}{l_c}\right)^2 \left[\left(W_{x_c}\,u(x_c)\right)^2 + \left(W_{x_c}^{cal}\,u(x_c)\right)^2\right] \\ &+ \left(\frac{L_p}{l_p}\right)^2 \left[\left(W_{x_p}\,u(x_p)\right)^2 + \left(W_{x_p}^{cal}\,u(x_p)\right)^2\right] \\ &+ \left(W_{x_R}^{cal}\,u(x_a)\right)^2 + \left(W_{z_R}^{cal}\,u(z_a)\right)^2 \Bigg\}^{1/2} \end{aligned} \quad (7b)$$

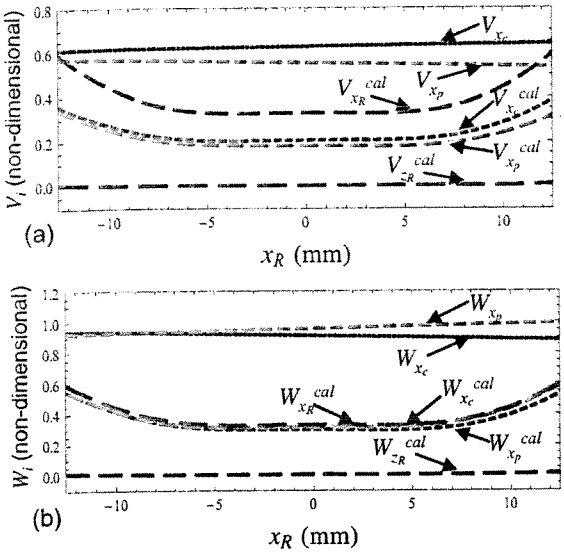

FIGURE 4. Plots of how sensitivities vary with workpiece position. a) V_i and b) W_i.

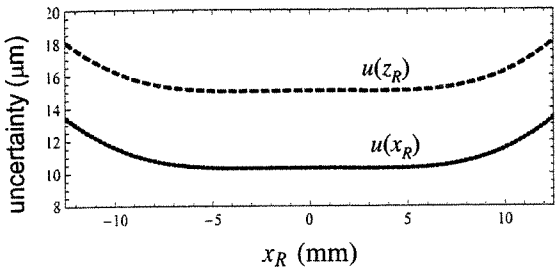

FIGURE 5. Variation of combined standard uncertainty in real-world coordinates with position on the workpiece.

than 30 known coordinates, and a higher density of known coordinates near the edges of the part might be ideal.

When the current analysis is expanded to three output dimensions, y-coordinates will be added to the camera, projector, and real-world. Also, in addition to the rotation about the y-axis already accounted for (θ in Fig. 1), rotations about the modified x- and z-axes will be included. The main concern with expansion is the added computational costs. Changes may be needed in the programming approach made to alleviate excessively long computation times.

CONCLUSION

We have conducted an uncertainty analysis of a simple fringe projection setup. This uncertainty analysis presented an interesting challenge in determining uncertainty due to the calibration process. To address this problem and to ensure

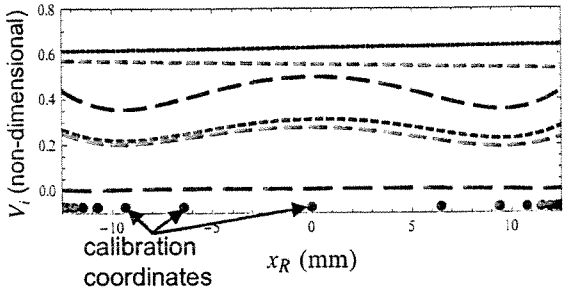

FIGURE 6. Variation of sensitivities with position on the workpiece resulting from re-distribution of the 30 calibration coordinates (blue dots).

all input quantities were independent, transformation matrix components were left in equation form and substituted into the measurement equation. In the end, the sensitivity coefficients, and therefore the combined standard uncertainties, were found to vary with position on the workpiece. The combined standard uncertainties in the output quantities $u(x_R)$ and $u(z_R)$ range from 10 μm to 18 μm.

ACKNOWLEDGEMENT

The authors would like to thank William Guthrie of the NIST Statistical Engineering Division for the insightful discussions regarding the current uncertainty analysis.

REFERENCES

[1] Batlle, J., Mouaddib, E., and Salvi, J., 1998, "Recent progress in coded structured light as a technique to solve the correspondence problem: a survey," *Pattern Recognition*, 31: 963-982.

[2] Salvi, J., Pages, J, and Batlle, J., 2004, "Pattern codification strategies in structured light systems," *Pattern Recognition*, 37: 827-849.

[3] Posdamer, J.L. and Altschuler, M.D., 1982, "Surface measurement by space-encoded projected beam systems," *Computer Graphics and Image Processing*, 18: 1-17.

[4] Tsai, M.-J. and Hung, C.-C., 2005, "Development of a high-precision surface metrology system using structured light projection," *Measurement*, 38: 236-247.

[5] Slama, C. (ed.), 1980, *Manual of Photogrammetry*, American Society of Photogrammetry, Virginia, USA.

[6] ISO, 2008, *Guide to the Expression of Uncertainty in Measurement*, Geneva, Switzerland.

where $u(x_c)$ and $u(x_p)$ are the standard uncertainties in camera and projector coordinates, and $u(x_a)$ and $u(z_a)$ are the standard uncertainties in the known points on the calibration artifact. The non-dimensional sensitivity coefficients (V_i and W_i) are complicated functions of camera, projector, and calibration artifact coordinates. Additionally, the sensitivity coefficients have been separated into those depending on the calibration artifact (superscript "cal") and those with no dependence on calibration (no superscript). This was done to ease calculations but also to aid understanding of the importance of the calibration to the combined standard uncertainty. L_c, l_c, L_p, and l_p are distances relative to the focal points of the camera and projector (see Fig. 1).

RESULTS

To evaluate the sensitivities, values specific to the geometry of the NIST system (see Fig. 2) were substituted into the equations for the sensitivity coefficients. The calibration artifact had uniform spacing of the known coordinates at two distinct heights (see Fig. 3). The results showed that the sensitivities vary with position on the workpiece, meaning different values of x_R and z_R have different sensitivities. However, because the workpiece height is very small compared to the camera and projector working distances, $z_R \approx 0$. Different values of x_R, however, remain significant. Figure 4 shows sensitivities across the workpiece. All sensitivities are rather uniform toward the center of the workpiece, but the sensitivities dependent on the calibration increase near the edges of the workpiece.

With the sensitivity coefficients evaluated, standard uncertainty values were substituted into Eqs. (7), yielding the combined standard uncertainties in the output quantities. The type B standard uncertainty in calibration artifact coordinates ($u(x_a)$ and $u(z_a)$) was assumed to equal 15 μm. The type A standard uncertainty in camera coordinates ($u(x_c)$) was 2 μm. The uncertainty in projector coordinates ($u(x_p)$) comes from the projector resolution. Therefore, it is a type B uncertainty dependant on the size of one projector pixel. For the current projector, this standard uncertainty was 6 μm. The resulting combined standard uncertainties are $u(x_R) \approx 10$ μm and $u(z_R) \approx 16$ μm near the center of the workpiece. Since the sensitivity coefficients increase toward the edges of the part, standard uncertainties also increase toward the edges (see Fig. 5).

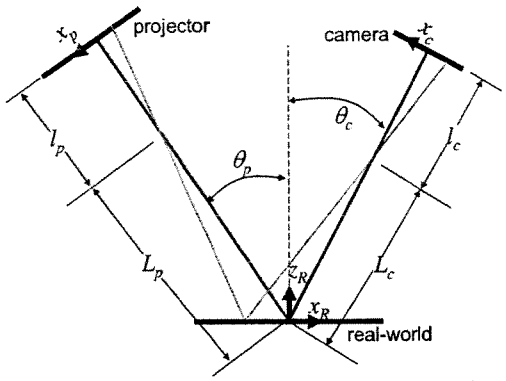

FIGURE 1. Schematic of fringe projection system analyzed in this study. Pinhole models describe both the camera and projector.

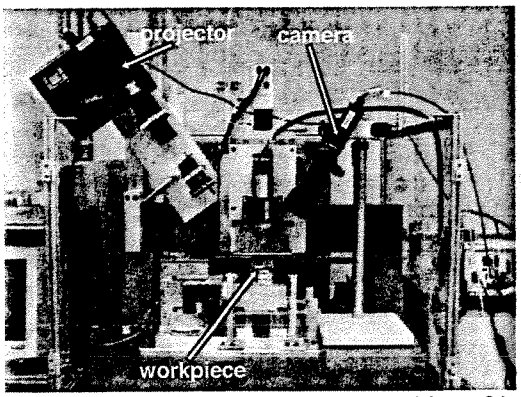

FIGURE 2. Photo of the on-machine fringe projection setup at NIST. For this setup, L_c = 350 mm, l_c = 66 mm, L_p = 425 mm, l_p = 215 mm, θ_c = 0.53 rad, and θ_p = 0.60 rad.

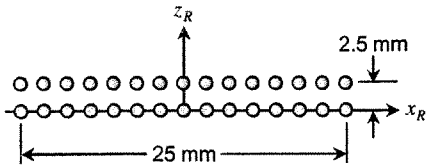

FIGURE 3. Model of a calibration artifact with 30 known coordinates.

LOOKING FORWARD

The uncertainty analysis can provide a useful tool to help improve the current fringe projection system. Because the uncertainty analysis reveals the importance of calibration to the combined standard uncertainty, the calibration artifact can be redesigned and evaluated. For example, redistributing the 30 known calibration points toward the workpiece edges, as shown in Fig. 6, slightly reduces sensitivities near the edges compared to those in Fig. 4(a), but at the expense of larger sensitivities near the center of the part. As such, a calibration artifact with more